Int J Fatigue **11** No 5 (1989) pp 341–346

Fatigue and fracture of a zinc die casting alloy

C.S. Shin and N.A. Fleck

The fracture toughness and crack tearing response were measured for a common zinc die casting alloy, BS1004: 1972 Alloy A. Its fatigue crack growth behaviour was also examined for constant amplitude loading and for a single overload. The constant amplitude crack growth rate was dependent upon both the effective stress intensity range ΔK_{eff} and the mean load of the fatigue cycle. Crack growth rates were faster than those in aluminium or in typical steels, when compared on the basis of $\Delta K/E$ or $\Delta K_{eff}/E$. These unusual features of the zinc alloy are due to its limited number of slip systems and susceptibility to cleavage. A tensile overload induces a transient retardation of fatigue crack growth rate. The primary cause of the retarded growth was found to be plasticity induced crack closure.

Key words: zinc die casting alloy; fracture toughness; crack propagation; crack closure

Most studies on static and cyclic fracture have been carried out on metals with the face centred cubic structure (*eg* aluminium alloys, nickel alloys and austenitic stainless steels) or the body centred cubic structure (*eg* low alloy steels). Relatively little is known about the fatigue and fracture behaviour of metals with a hexagonal close packed (HCP) structure. In particular, there is no previous work known to the authors on fatigue crack growth in zinc alloys, which possess a HCP structure and a limited number of slip systems.

In this paper, the fatigue crack propagation response and fracture toughness of the 4%-aluminium zinc die casting alloy BS1004: 1972 Alloy A is investigated. Fatigue crack growth is characterized in terms of the stress intensity range ΔK and the crack closure response for the case of constant amplitude loading and also for a single tensile overload. The zinc alloy BS1004: 1972 Alloy A is commonly used for castings made by the hot chamber pressure die casting process; these castings usually fail by fatigue and brittle fracture rather than by plastic collapse.

Material and specimen geometry

Compact tension (CT) specimens of width 50 mm and notch length 15 mm were machined from 3.2 mm thick zinc alloy castings. The zinc alloy conforms to British Standard BS1004: 1972 Alloy A and has a nominal percentage composition by weight of 3.8–4.3 Al, 0.03–0.06 Mg, remainder Zn. The zinc alloy castings have a measured yield stress, σ_y, of 210 MPa, ultimate tensile stress of 285 MPa, elongation on 50 mm of 15% and a Young's modulus, E, of 73 GPa, at a strain rate of 10^{-3} s^{-1}.

The 3.2 mm thick specimens were used to determine the fracture toughness and fatigue crack propagation (FCP) response of the zinc alloy. In addition, tests were performed on CT specimens made from a 1.6 mm thick casting to determine the effect of thickness on FCP behaviour.

Fracture toughness tests

Preliminary measurements indicated that a specimen has to be at least 25 mm thick for a valid measurement of the plane strain fracture toughness K_{IC}, in accordance with ASTM E399–81. The maximum available thickness is 3.2 mm. Fortunately, the J-integral test procedure is valid, as specified in ASTM E813–81.

Measurements of J_{IC} toughness were performed using the single specimen technique, see ASTM E813–81 for details. Compact tension specimens of thickness 3.2 mm were fatigue pre-cracked using a stress intensity range ΔK of 8 MPa $m^{1/2}$ and load ratio R (equal to minimum load/maximum load) of 0.05. During the toughness test, the crack length was measured using a travelling microscope, rather than relying upon the indirect method of unloading compliance. Fractographic examination confirmed that the crack front remained straight throughout the test, thus surface measurements of crack length are valid.

Results and discussion

The J-integral versus crack extension, Δa, response was calculated from the load, P, versus crack opening displacement, v, response of a specimen, as specified in ASTM E813–81. The displacement, v, is measured along the load line by mounting a clip gauge across the notch, on one side face of the specimen.

Results are given in Fig. 1 for three different initial crack length-to-width ratios, ranging from 0.52 to 0.67. A least square fit through the J-Δa crack tearing data gives a linear regression line which intercepts the blunting line $J = 2\sigma_y \Delta a$ at $J_Q = 4.5 \times 10^{-3}$ MNm^{-1}. The quantity $25 J_Q/\sigma_y = 0.56$ mm is less than both the specimen thickness (3.2 mm) and the minimum initial ligament size (16.4 mm). Also, the slope of the regression line is 18 MPa, which is less than the yield stress (210 MPa). Thus J_Q is a valid measure of the

0142-1123/89/030341–06 $3.00 © 1989 Butterworth & Co (Publishers) Ltd

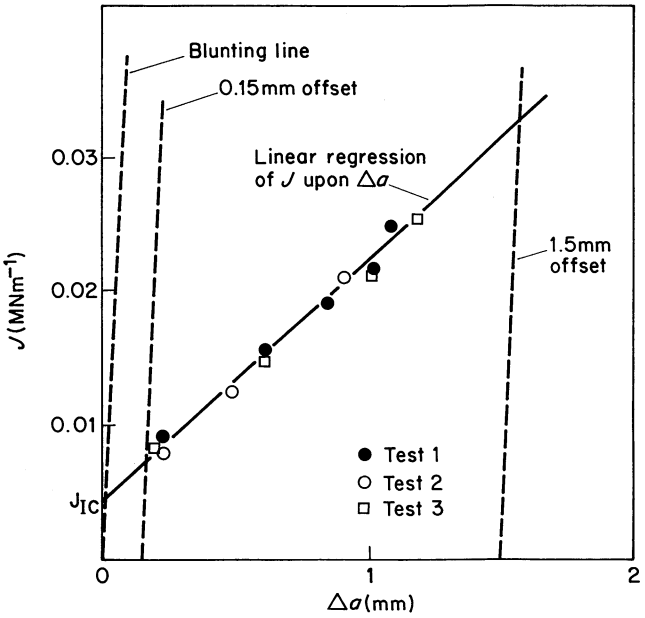

Fig. 1. Crack tearing response J–Δa for 3.2 mm thick specimens

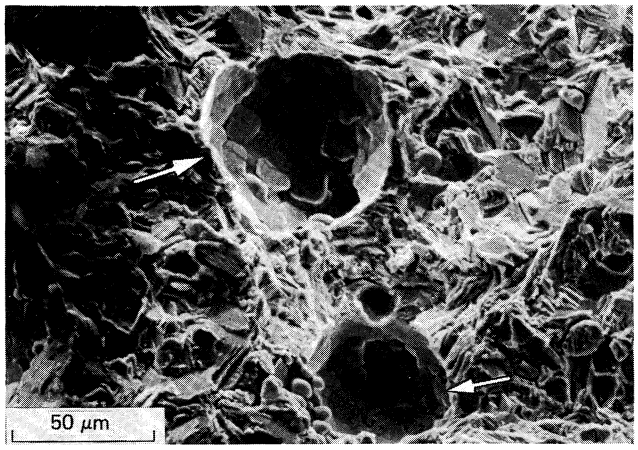

Fig. 2. Fracture surface due to static loading. Crack growth direction is from the bottom to the top of the micrograph. The arrows indicate large pores produced during casting

plane strain toughness and can be designated J_{IC}. The corresponding plane strain fracture toughness $K_{IC} = \bar{E}J_{IC}^{1/2}$ is 18.5 MPa $m^{1/2}$, where $\bar{E}$ is the plane strain Young's modulus.

The scatter in the J-Δa response, Fig. 1, is partly due to the fact that the material contains a random distribution of pores, as shown on the fracture surface, Fig. 2. Crack advance is by transgranular cleavage of the primary Zn rich β dendrites, and of the eutectoid (α + β) mixture between the dendrites. There is no evidence of ductile fracture by hole growth. The fracture surface contains many pores and is rough to the naked eye, with a centreline-average roughness of 33 μm and a peak–peak roughness of 0.70 mm on a traverse length of 2 mm. It is thought that crack advance occurs along the weakest path from pore to pore.

The zinc alloy is susceptible to cleavage as the zinc rich β phase contains insufficient slip systems to accommodate plastic flow and deforms by twinning in addition to slip.

Fatigue crack propagation tests

The fatigue crack growth and crack closure responses were determined for both constant amplitude loading and for a single overload. Crack length was measured with a travelling microscope, and the crack closure response was monitored by an offset compliance technique using a back face strain gauge. Crack closure was quantified by the U value, defined as the fraction of the load cycle for which the crack is open. Thus

$$U = \frac{(K_{max} - K_{op})}{(K_{max} - K_{min})} = \frac{\Delta K_{eff}}{\Delta K}$$

where K_{max}, K_{min} and K_{op} are the maximum, minimum and crack opening stress intensities, respectively.

Both crack length and crack closure measurements were taken at the test frequency of 5 Hz.

Constant amplitude tests

The influence of specimen thickness and mean load upon crack growth rate were determined using constant amplitude loading with a sinusoidal waveform. The 3.2 mm thick specimens suffered a load ratio, R (equal to minimum load/maximum load), of 0.05 and 0.5, while the 1.6 mm thick specimens suffered a load ratio, R, of 0.05 only. Results in the form of crack growth rate, da/dN, versus stress intensity range, ΔK, are shown in Fig. 3.

There is no significant difference in crack growth rate between the thick and thin specimens for the same load ratio of 0.05, to within the experimental scatter. The main cause of scatter is probably the random porosity, leading to local crack accelerations and retardations. The density of the specimens varies from 6390 kgm^{-3} to 6630 kgm^{-3}, while the density of the fully dense material is 6940 kgm^{-3} by a calculation based on the chemical composition. Thus the porosity is in the range 4.5–7.9%. It is clear from Fig. 3 that

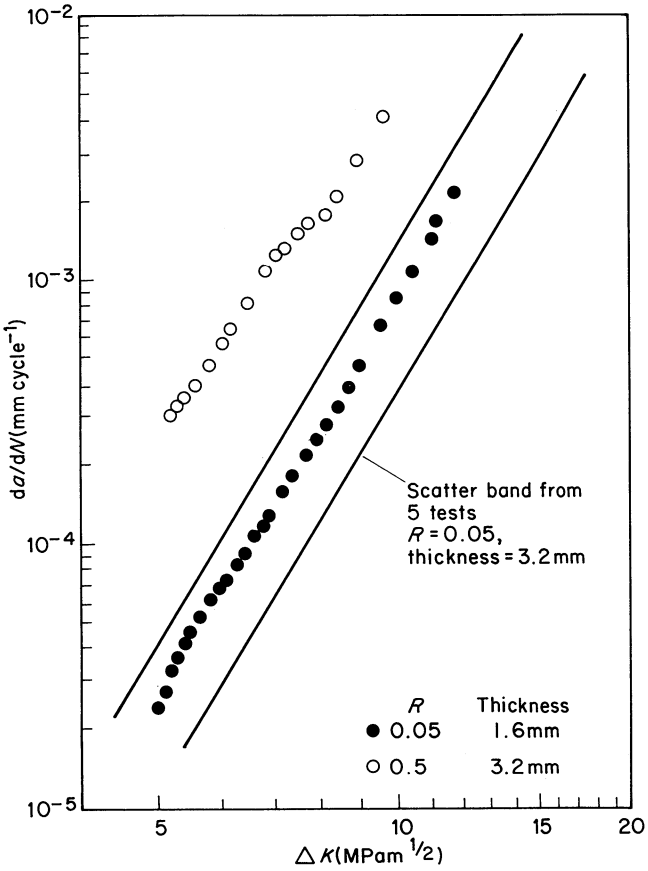

Fig. 3. Crack growth rate da/dN versus stress intensity range ΔK for R = 0.05 and R = 0.5

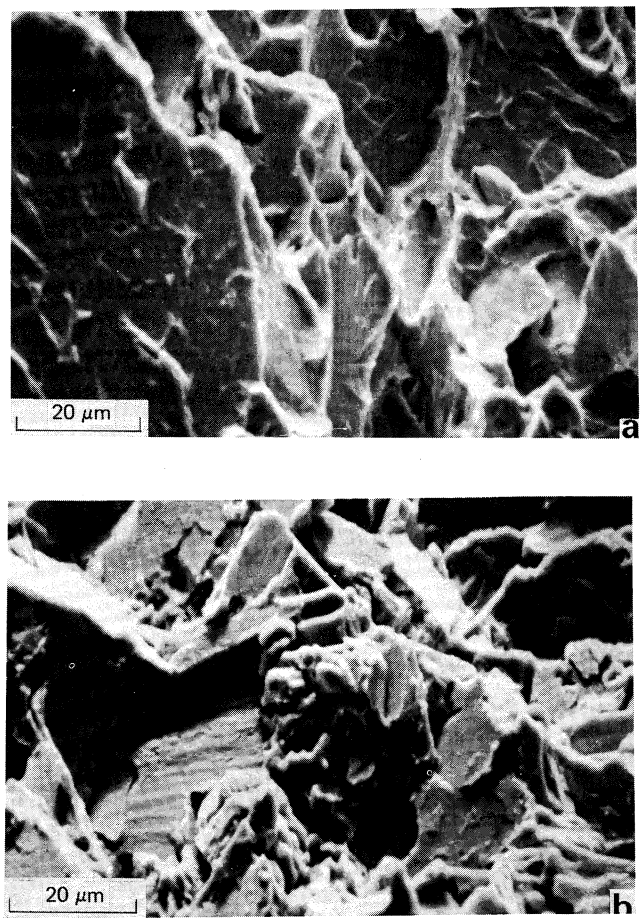

Fig. 4. Fatigue fracture surfaces for (a) R = 0.05 and (b) R = 0.5. In both cases crack growth is from bottom to top of the micrograph at 3 × 10^{-3} mm cycle^{-1}

the crack growth rate is sensitive to mean load; the crack propagation rate increases by an order of magnitude as the load ratio, R, is increased from 0.05 to 0.5 under the same ΔK.

Typical fatigue fracture surfaces of the 3 mm thick specimens for R = 0.05 and R = 0.5 are shown in Fig. 4. For both R values there is a large area fraction of transgranular cleavage of the zinc rich β dendrites. The dominance of this static fracture mode may account for the higher growth rate at the higher R value.

The roughness of the fatigue fracture surface is about 9 μm centreline-average, compared with 33 μm for the static fracture surface. This suggests that the crack is less prone to follow the path of maximum porosity under fatigue loading than under static loading.

Crack closure measurements

For the tests with a load ratio R, of 0.05, the fraction of the load cycle for which the crack is open, U, increases from 0.75 to 0.85 as ΔK is increased from 5 MPa m$^{1/2}$ to 15 MPa m$^{1/2}$. At R = 0.5, the crack remains open during the whole loading cycle. This is consistent with evidence of abrasion on the fracture surface for R = 0.05 but not for R = 0.5

The crack growth rate is plotted as a function of the effective stress intensity range $\Delta K_{eff} = U\Delta K$ in Fig. 5. The data for the thick and thin specimens at R = 0.05 lies in a scatter band of the same width as that in Fig. 3. However, the effect of R on growth rate is much reduced when a comparison is based on ΔK_{eff}, Fig. 5, rather than ΔK, Fig.

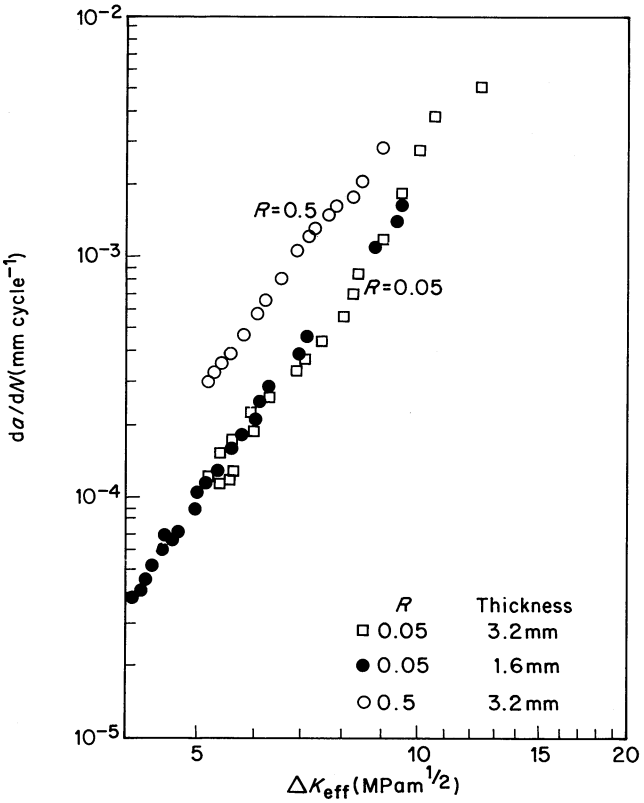

Fig. 5. Crack growth rate da/dN versus effective stress intensity range ΔK_{eff} for R = 0.05 and R = 0.5

3. Under the same ΔK_{eff}, the growth rate at R = 0.5 is about twice that at R = 0.05.

In view of the existence of a static failure mode by transgranular cleavage of the β dendrites, the maximum stress intensity factor, K_{max}, may be an appropriate parameter to describe the crack driving force. Fig. 6 shows such a rationalization. Under the same K_{max}, the growth rate at R = 0.5 is now less than that at R = 0.05 by a factor of about two.

It is concluded from Figs 5 and 6 that the crack growth rate is dependent upon both ΔK and K_{max}. Under the same ΔK_{eff}, both K_{max} and the crack growth rate are higher for R = 0.5 than for R = 0.05. On the other hand, under the same K_{max}, both ΔK_{eff} and the crack growth rate are higher for R = 0.05 than for R = 0.5.

Crack growth rate comparison with other materials

It has been observed[1] that fatigue crack propagation data in various metallic alloys can be rationalized by $\Delta K/E$, and even more successfully by $\Delta K_{eff}/E$.[2] In Fig. 7, fatigue crack growth data are compared on the basis of $\Delta K/E$ for the zinc alloy, a commercially pure aluminium, AISI 316 stainless steel and BS4360 50B structural steel. All the data relate to a load ratio, R, of 0.05. The zinc alloy has a hexagonal close packed structure, the aluminium and stainless steel have a face centred cubic structure and the structural steel is primarily ferrite with a body centred cubic structure. It is apparent from Fig. 7 that the crack growth rate of the zinc alloy is higher than that of the other materials under the same $\Delta K/E$. This is even more pronounced if the parameter $\Delta K_{eff}/E$ is used instead of $\Delta K/E$, see Fig. 8.

The faster growth rate in the zinc alloy may be due to the fact that it has a hexagonal close packed structure with a

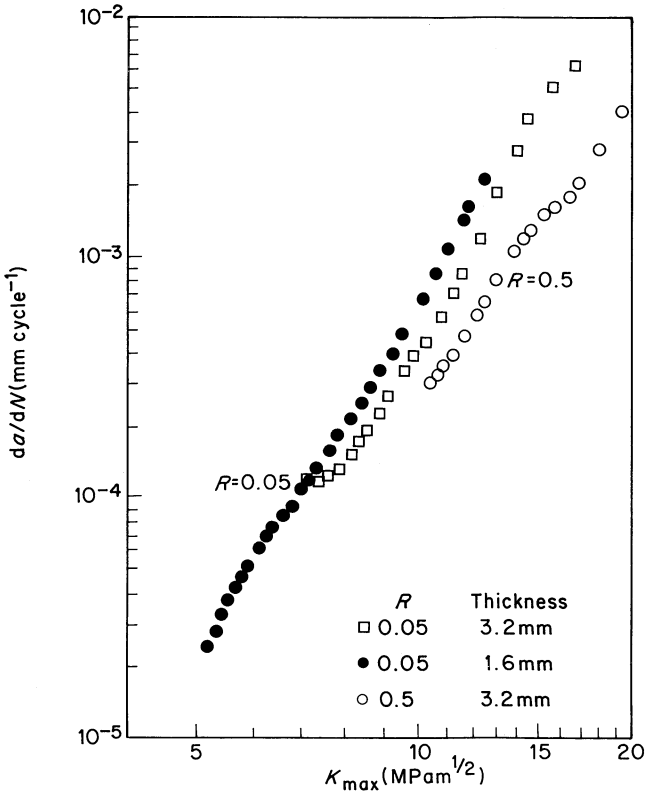

Fig. 6. Crack growth rate da/dN versus maximum stress intensity factor K_{max} for R = 0.05 and R = 0.5

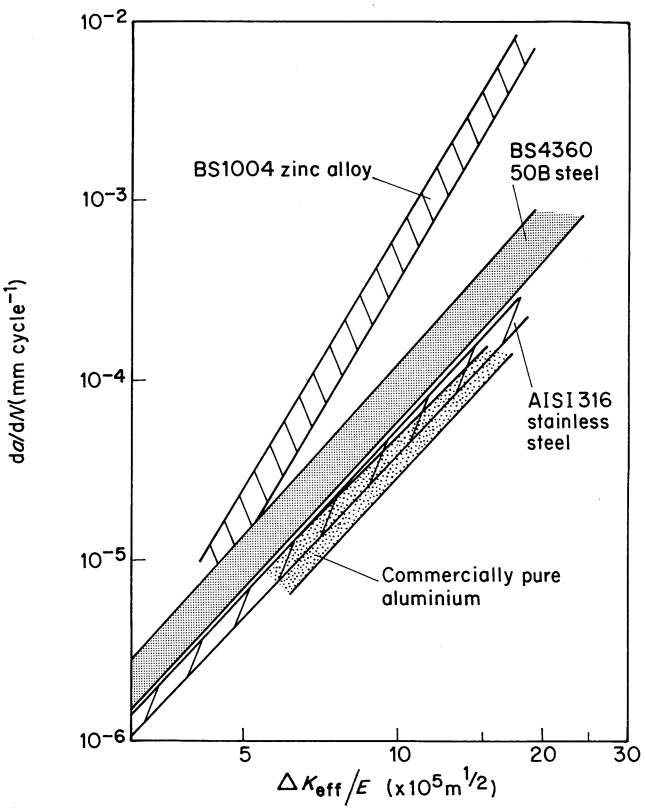

Fig. 8. Comparison of crack growth rates for a variety of metallic systems, on the basis of $\Delta K_{eff}/E$. In all cases R = 0.05

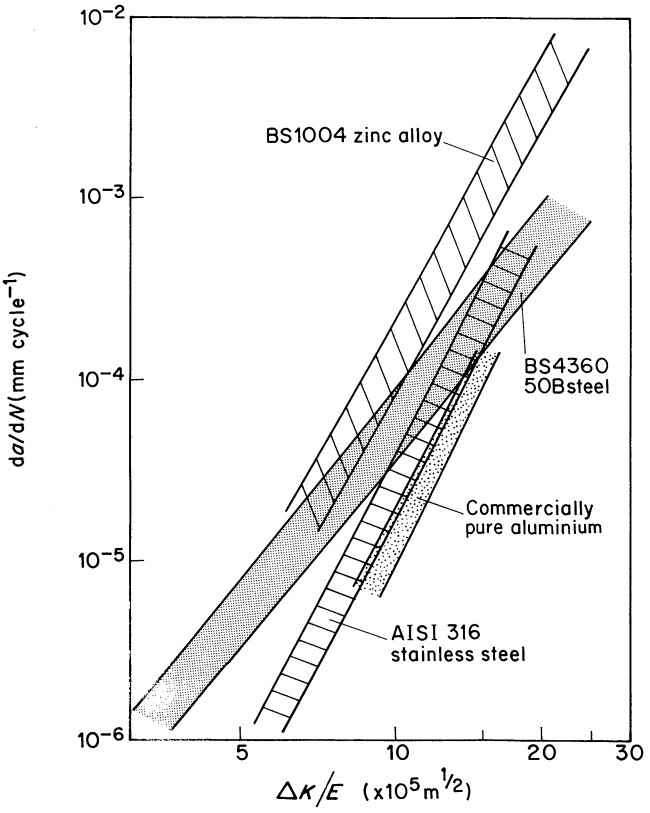

Fig. 7. Comparison of crack growth rates for a variety of metallic systems on the basis of $\Delta K/E$. In all cases R = 0.05

limited number of slip systems; fatigue crack growth is accompanied with extensive static fracture by cleavage. In contrast, the steels and aluminium have an adequate number of slip systems. The scatter bands in crack growth for the aluminium and steels become parallel and closer together when plotted against $\Delta K_{eff}/E$ rather than $\Delta K/E$, as expected on the basis of crack closure arguments.

Mechanisms of crack closure in the zinc alloy

At a load ratio of 0.05, a fatigue crack in the zinc alloy is shut during part of the load cycle. The most likely mechanism of crack closure for this material and for the growth rates considered is plasticity induced crack closure. Roughness induced crack closure is also significant: the crack tip opening displacement, $\delta = K_{max}^2/\sigma_y E$ is in the range 1–20 μm for the stress intensities considered while the typical centreline-average roughness of the fatigue fracture surface is 9 μm. Hence asperity–asperity contact is likely.

To confirm that crack closure has a significant influence on crack growth rate a specimen was stress relieved as follows. After growing a crack for 7 mm at a constant ΔK = 7.5 MPa m$^{1/2}$ and R = 0.05, the load was reduced to zero. The specimen was stress relieved *in-situ* by maintaining it at 90°C for 4 h using an infrared lamp. This operation allows residual stresses associated with plasticity and roughness induced crack closure to be relieved, but has little effect upon the geometry of the fracture surfaces. After stress relief, the same constant ΔK loading was resumed and the crack was grown for a further 6 mm. Results in the form of the crack growth and crack closure responses are shown in Figs 9 and 10, respectively.

Immediately after stress relief the crack growth rate shows a discontinuous jump to twice the steady state value. Concurrently, the U-value increases from 0.75 to unity,

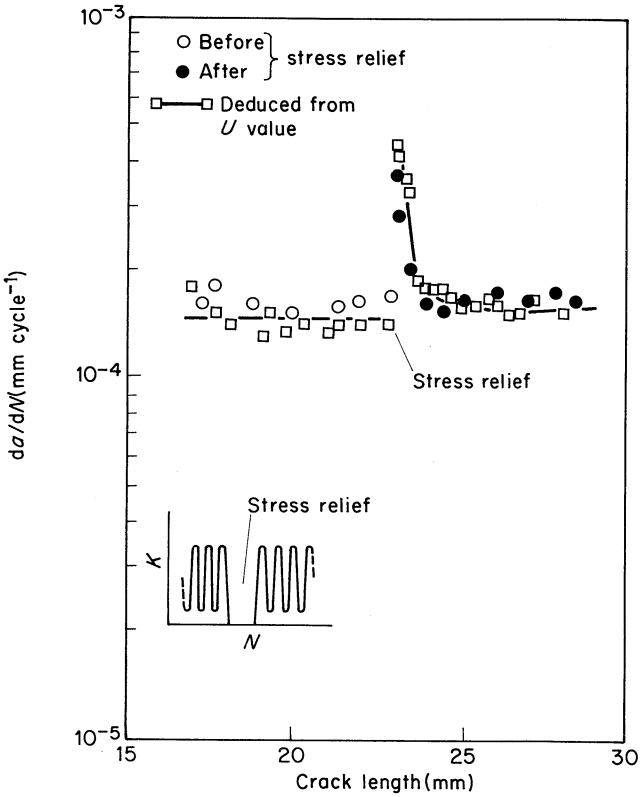

Fig. 9. Comparison of measured and predicted crack growth rates following a stress relief operation

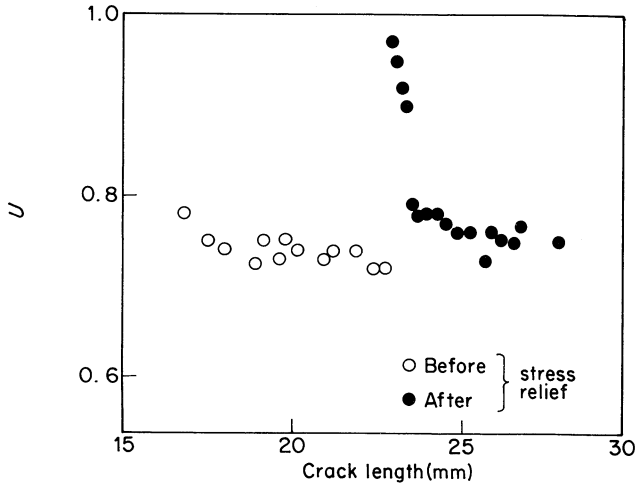

Fig. 10. Fatigue crack closure transient following a stress relief operation

indicating removal of crack closure. With subsequent crack growth the crack growth rate and closure response recover their steady state values.

From the closure response shown in Fig. 10 the associated ΔK_{eff} history can be calculated, and the corresponding crack growth rate can be deduced from the da/dN versus ΔK_{eff} response at $R = 0.05$ given in Fig. 5. The predicted growth rates agree well with the measured values, see Fig. 9. It is concluded that the crack growth transient immediately following the stress relief operation can be explained in terms of crack closure, and that the crack growth rate in low R-ratio tests is significantly influenced by crack closure.

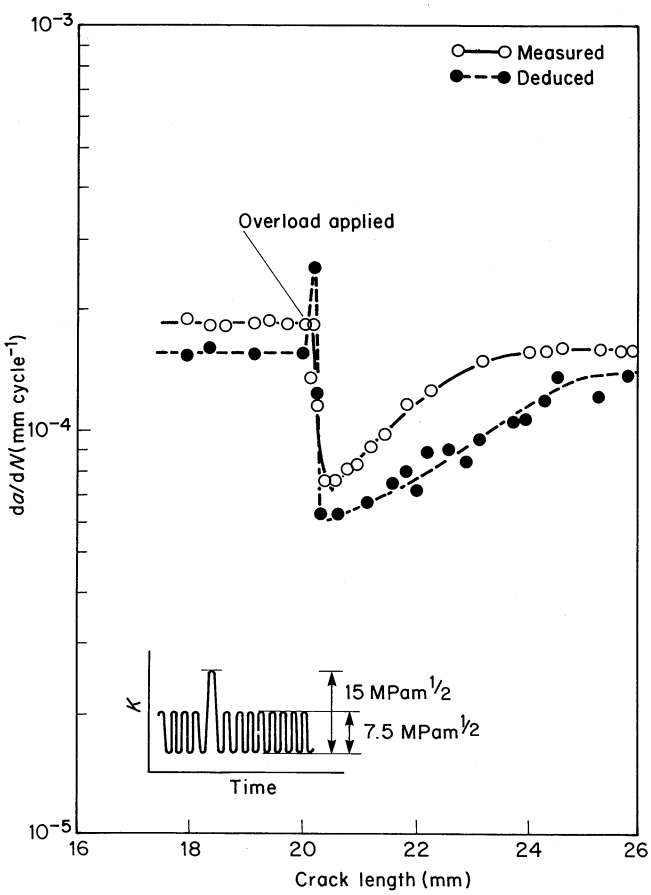

Fig. 11. Comparison of measured and predicted crack growth rates following an overload

Effect of an overload on fatigue crack growth rate

A test was performed on a 3.2 mm thick specimen to examine whether crack closure is able to account for crack growth retardation following an overload. First, a crack was grown at a constant baseline stress intensity range $\Delta K_b = 7{\cdot}5$ MPa $m^{1/2}$ and $R = 0.05$ from the starter notch. This loading is sufficiently low for plane strain conditions to prevail along most of the crack front. To obtain a constant ΔK_b, the crack length was measured using a DC potential drop system and the load was shed automatically after crack growth increments of 0.2 mm using a microcomputer. After 5 mm of growth, an overload of range twice ΔK_b was applied, and the baseline loading was then resumed. The associated crack growth transient is shown in Fig. 11.

Comparison of surface measurements of crack length with potential drop measurements indicates that the crack front remained straight throughout the test. Prior to the overload, the crack grew at a constant rate of 1.8×10^{-4} mm $cycle^{-1}$. On application of the overload, deformation bands appeared, of length 0.05 mm and at angles of $\pm$ 45° to the cracking plane. After resumption of the baseline loading, the crack grew in a self-similar direction without any branching. The growth rate remained constant for a crack growth increment of 0.1 mm; the crack then retarded to a minimum growth rate of 7.4×10^{-5} mm $cycle^{-1}$ at a location of 0.5 mm ahead of the overload location. Finally, the growth rate accelerated back to the pre-overload value when the crack had grown about 5 mm from the overload position.

The fatigue crack closure response is considered next. On application of the overload, the crack closure value U

jumped discontinuously from its steady state pre-overload value of 0.75 to 0.85. It then decreased rapidly to a minimum value of 0.60 after a growth increment of 0.5 mm from the overload position. Inferred crack growth rates are calculated from the measured closure values and the da/dN versus ΔK_{eff} response at $R = 0.05$, see Fig. 5. The inferred growth rates are in reasonable agreement with the measured growth rates, see Fig. 11, except for the period when the growth rates are recovering from the minimum post-overload value to the steady state response. During this period, the measured growth rates are greater than the predicted rates. It is thought that this is due to discontinuous closure, as has been observed for a medium strength structural steel:[3,4] after some crack growth from the overload location, the crack closes first at a position far from its tip and suffers a cyclic crack opening at loads below the closure load. The predicted growth rate is then less than the measured rate. The phenomenon is due to the large plastic stretch given to the material by the overload.

It is concluded that crack closure is able to account for the retardation in crack growth rate following an overload once discontinuous closure is taken into account. The retardation in crack rate for the zinc alloy is little more than a factor of 2. By comparison, the crack growth rate in steels and aluminium alloys is retarded typically by more than an order of magnitude for an overload of 2 and a pre-overload growth rate of 10^{-4} mm cycle^{-1}.[3–6] The much smaller retardation in the zinc alloy is consistent with the fact that near crack tip straining in the zinc alloy is by a combination of slip, twinning and cleavage microcracking.

Conclusions

- The J-integral method has been used successfully to determine the fracture toughness of 3.2 mm thick specimens made from a zinc alloy, BS1004: 1972 Alloy A. Static crack growth is predominantly by cleavage.
- Fatigue crack growth in the zinc alloy is accompanied by crack closure when the load ratio equals 0.05. No closure is observed at a load ratio of 0.5. The driving force for fatigue crack growth is a combination of ΔK_{eff} and K_{max}. This is consistent with the observation that cleavage contributes significantly to fatigue crack growth. The zinc alloy displays faster crack growth rates than aluminium or two typical steels when compared on the basis of $\Delta K/E$ or $\Delta K_{eff}/E$.
- Fatigue crack retardation following an overload in the zinc alloy is primarily due to crack closure. It is thought that the apparent discrepancy between measured growth rates and the predicted growth rates from closure measurements is due to discontinuous closure.

Acknowledgements

The authors would like to thank Dr J.M. Birch of the Zinc Alloy Die Casters Association for provision of test materials.

References

1. **Bates, R.C. and Clark, W.J. Jr.,** *Trans Quart ASM* **62** 2 (1969) p 380
2. **Liaw, P.K., Leax, T.R. and Logsdon, W.A.** 'Near-threshold fatigue crack growth behaviour in metals' *Acta Met* **31** 10 (1983) pp 1581–1587
3. **Fleck, N.A.** 'Influence of stress state on crack growth retardation, ASTM STP 924' in *ASTM Workshop on Basic Questions in Fatigue, Vol I* (eds J.T. Fong and R.J. Fields) (American Society for Testing and Materials, 1988)
4. **Fleck, N.A., Smith, I.F.C. and Smith R.A.** 'Closure behaviour of surface cracks' *Fatigue Engng Mater Struct* **6** 3 (1983) pp 225–239
5. **Chanani, C.R.** 'Effect of thickness on retardation behavior of 7075 and 2024 aluminium alloys' in *Flaw Growth and Fracture, ASTM STP 631* (American Society for Testing and Materials, 1977) pp 365–387
6. **Gallagher, J.P. and Hughes, T.F.** 'Influence of yield strength on overload affected fatigue crack growth behaviour in 4340 steel' *Wright-Patterson Air Force Base, AFFDL-TR-74-27* (1974)

Authors

C.S. Shin is with the Materials Research Laboratories, 195–5, Section 4, Chung Hsing Road, Chu-Tung, Hsinchu, 3105, Taiwan, Peoples Republic of China. N.A. Fleck is with the Department of Engineering, University of Cambridge, Trumpington Street, Cambridge, CB2 1PZ, UK.